Hindawi
Geofluids
Volume 2022, Article ID 8083443, 13 pages
https://doi.org/10.1155/2022/8083443

Research Article

Failure Mechanism and Acoustic Emission Precursors of Coal Samples considering Bedding Effect under Triaxial Unloading Condition

Rui Yang[1], **Yan Zhou**[2] and **Depeng Ma**[1,3]

[1]*Shandong Key Laboratory of Civil Engineering Disaster Prevention and Mitigation, Shandong University of Science and Technology, Qingdao 266590, China*
[2]*College of Information Science and Engineering, Shandong Agricultural University, Taian 271018, China*
[3]*College of Water Conservancy and Civil Engineering, Shandong Agricultural University, Taian 271018, China*

Correspondence should be addressed to Yan Zhou; zhouyansdust@163.com and Depeng Ma; mdp123@163.com

Received 6 April 2022; Revised 17 June 2022; Accepted 28 June 2022; Published 3 August 2022

Academic Editor: Dongjiang Pan

Bedding increases coal seam anisotropy, which leads to significant differences in the evolution laws of mining stress and strata movement. This work analyzed the dip angles of different layers to analyze the mechanical properties of the coal seam under unloading. The coal sample was subjected to triaxial compression and unloading damage acoustic emission testing. The brittleness characteristics of the coal sample failure in different bedding directions differed significantly. Compared with axial parallel bedding coal samples, axial vertical bedding and inclined stratification reached an ultimate strength. The stress–strain curve decreased sharply and showed visible brittle-drop characteristics. The average strengths of the axially inclined bedding and the parallel layered coal sample decreased compared with the axial vertical bedding coal sample and were 10.20 and 16.12 MPa, respectively, which implies a greater susceptibility to failure during unloading confining pressure tests. Acoustic emission monitoring indicated that the axial vertical bedding and inclined bedding showed sudden destruction of different coal samples, a reduction in axial parallel bedding ductility coal sample characteristics, and stronger unloading damage on the axis parallel to the bedding coal sample. Further, using the acoustic emission ring count rate and the cusp catastrophe theory, the unloading failure prediction of coal samples is carried out. The prediction results are not different from the experimental results, which shows that this method is feasible.

1. Introduction

In a diagenetic environment with different climates and compositions, many weak structural surfaces result during coal formation, such as voids and beddings, which contribute to the physical and mechanical property heterogeneity. Beddings affect coal heterogeneity most.

As a result of the geological structure, various beddings are encountered from different angles during coal mining, such as horizontal, oblique, and even vertical beddings, which promote coal seam anisotropy and lead to considerable differences in mining-induced stress and the development law of the overburden. This phenomenon is termed the bedding effect, as shown in Figure 1.

The bedding effect has received extensive research attention. K.D. Liu et al. [1], X.H. Liu et al. [2], Xu et al. [3], and Hou et al. [4, 5] conducted Brazilian splitting tests on coal and shale samples considering the bedding effect and analyzed the deformation and strength characteristics of bedding rock mass under indirect tension. Teng et al. [6, 7] and Ren et al. [8] conducted uniaxial compression tests on bedding shale, anchored rock mass, and coal rock. They also analyzed the failure characteristics of bedding rock mass under uniaxial compression. Zhang et al. [9], Yang et al. [10], and Sun et al. [11] studied the impact of bedding angle on acoustic emission (AE) parameters of coal samples based on uniaxial compression AE test. Xie et al. [12] studied the impact of bedding on the dynamic mechanical failure

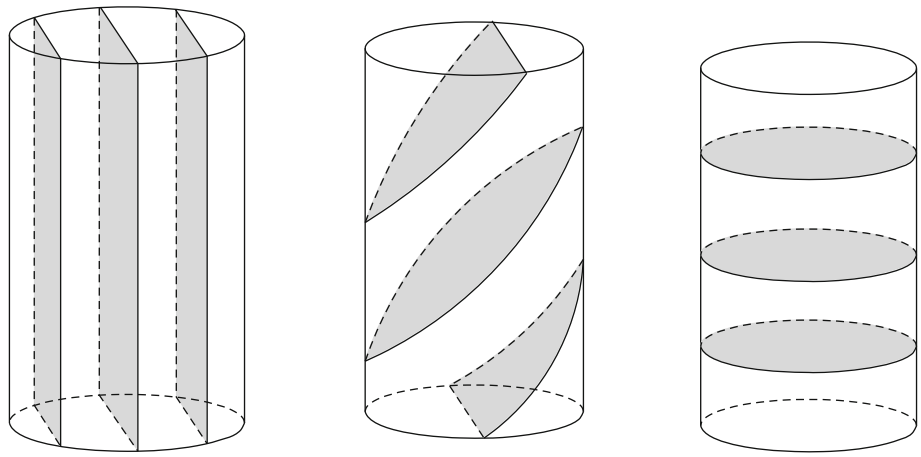

Figure 1: Schematic diagram of coal beddings.

characteristics of coal and sandstone based on the dynamic mechanical experiment. Pei et al. [13] analyzed the mechanical characteristics of layered marble under conventional triaxial loading and unloading conditions. Deng et al. [14] conducted uniaxial and triaxial compression tests on sandstone with seven bedding angles and analyzed the impact of the bedding angle on the mechanical properties and failure mode of rock mass. Li et al. [15] studied the impact of bedding on the reconstruction effect of the shale reservoir in the height direction based on a large-scale true triaxial fracturing simulation experiment. Liu et al. [16] tested the thermal expansion coefficient of bedding sandstone by using a rock expansion coefficient and investigated the variation law of the axial and radial thermal expansion coefficients of rock.

Since the discovery of acoustic emission in rocks in the 1930s, the application of acoustic emission technology in rocks has gradually developed. However, there are few studies on the evolution law of acoustic emission characteristics and fracture prediction of rocks (especially coal samples) under unloading. Such studies mainly focus on loading test of materials. Song et al. [17], Zhang et al. [18], Li et al. [19], and Liu et al. [20] studied the temporal and spatial evolution law of rock-like materials and constructed the corresponding constitutive equation. Zhang et al. [21], Yao et al. [22], and Zhang et al. [23] studied the relationship between acoustic emission parameters and energy under uniaxial compression and triaxial compression, as well as the judgment of fracture precursor information. Yang et al. [24] studied acoustic emission characteristics of coal under different triaxial unloading conditions. Therefore, it is feasible to study the temporal and spatial evolution law of rocks and rock-like materials based on acoustic emission parameters. However, the mechanical behavior of rock failure is extremely complex. It is difficult to fully and accurately describe the complex mechanical behavior of rock failure and its prediction only from the perspective of characterization parameters (ringing, impact, energy, etc.). Therefore, it is very necessary to further analyze the acoustic emission parameters in order to find the precursor parameters that can more comprehensively and accurately reflect the characteristics of rock unloading failure.

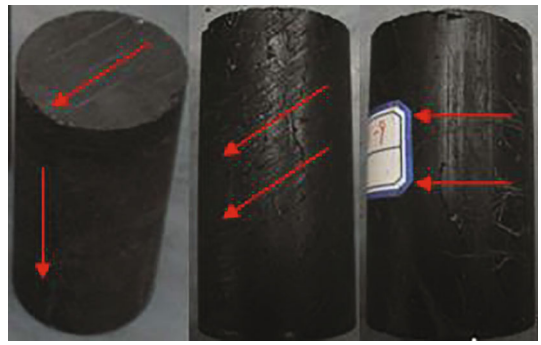

Figure 2: Standard prepared coal rock sample.

Extensive literature has focused on bedding characteristics of coal (or rock) in uniaxial compressive strength tests, triaxial compressive strength tests (TCSTs), and indirect tensile tests. However, the mechanical characteristics of coal under the influence of bedding effect have rarely been studied. In panel retreating, entry extraction, and other mining activities, rock mass occurs in the unloading state in most cases, which reduces the stress in a certain direction, and rock mass deformation and failure result. The peak strength of the coal sample has a significant effect under unloading conditions compared with loading conditions. Therefore, research on the mechanical characteristics of coal under the influence of bedding effect is of great importance in theory and practical application. Based on typical stratified coal samples in Yanzhou (China), this work focused on traditional triaxial compressive tests and the triaxial unloading tests (TUTs) with AE according to the evolution of stress of the surrounding rock of the panels in a coal mine to study the evolution law of mechanical characteristics of three coal sample types with bedding planes (see Figure 1) under an unloading condition. The failure and AE of the coal sample was analyzed when the main stress and bedding planes were at different angles.

2. Materials and Methods

2.1. Starting Material. Coal samples were collected from the No. 16 coal seam in the Yangcun Coal Mine, Jining,

Table 1: Experimental procedures.

Test categories	Loading type	Confining stress (MPa)	Unloading rate (MPa/s)	No.
TCST	V	10	—	V-S-1
TCST	V	10	—	V-S-2
TCST	V	10	—	V-S-3
TUT	V	10	0.05	V-X-1
TUT	V	10	0.05	V-X-2
TUT	V	10	0.05	V-X-3
TCST	T	10	—	T-S-1
TCST	T	10	—	T-S-2
TCST	T	10	—	T-S-3
TUT	T	10	0.05	T-X-1
TUT	T	10	0.05	T-X-2
TUT	T	10	0.05	T-X-3
TCST	P	10	—	P-S-1
TCST	P	10	—	P-S-2
TCST	P	10	—	P-S-3
TUT	P	10	0.05	P-X-1
TUT	P	10	0.05	P-X-2
TUT	P	10	0.05	P-X-3

Shandong, China. The coal seam texture was simple, with 1–2 local partings of a mudstone and pyrite lithology and a 0.02–0.44 m thickness. The coal block was cut into 50 mm diameter, 100 mm high cylinders according to engineering rock mass test standards. To ensure homogeneity, the coal samples were subjected to ultrasonic testing to provide a residual wave velocity of 1900–2000 m/s. As shown in Figure 2, the coal samples were divided into three groups (0°, 45°, and 90°) and numbered according to the angle between the bedding plane and the longitudinal direction; that is, the bedding plane was parallel (P), perpendicular to (V), and at an angle to (T) the longitudinal direction of the samples.

2.2. Experimental Procedures. Triaxial loading and unloading tests were performed by using the MTS815.02 electrohydraulic servo rock mechanics and the AE21C AE test systems, which meets requirements for a variety of complex paths. The experimental procedures were as follows.

2.2.1. Traditional Triaxial Compressive Test (TCST). TCSTs were performed with different confining pressures that were applied gradually to a setpoint (10 MPa) according to the hydrostatic pressure by stress control. The confining pressure was kept constant, and the axial pressure was increased by displacement control with a constant axial displacement loading rate (0.002 mm/s) until the sample failed.

2.2.2. Triaxial Unloading Test (TUT). The side abutment pressure of the coal body (which is equivalent to the confining pressure) decreased gradually during mining. The front abutment pressure (which is equivalent to the axial stress) increased. Panel retreating is a process with a reduction in confining pressure and an increase in axial pressure of the surrounding rock and coal body. Therefore, the experiment was carried out under an unloading path of an increase in axis pressure and a decrease in confining pressure. This unloading path is most dangerous with the shortest failure span.

Three stages occurred in the entire unloading experiment. (1) A gradual increase in confining pressure (σ_3) to a predetermined value (4, 7, or 10 MPa) according to the hydrostatic pressure conditions. (2) σ_3 was held constant while the axial pressure (σ_1) was increased to 80% of the compressive peak stress of the conventional triaxial tests using the stress control method. (3) The displacement control method was used to increase σ_1 while decreasing σ_3 simultaneously at 0.02, 0.05, 0.08, 0.11, or 0.14 MPa/s until sample failure, as shown in Table 1. The reduction in confining pressure stopped immediately after the specimen was damaged, while the axial pressure continued to load to the residual specimen strength using the displacement control method.

The AE monitoring system was used to monitor and collect information on the coal samples during the test, with the following parameters: sampling frequency, gain, and threshold of 10 MHz, 30 dB, and 35 dB, respectively.

3. Test Result Analysis

3.1. Stress–Strain Relationship. Figures 3 and 4 show the curves of the coal samples with different bedding directions in the traditional TCSTs and TUTs at a constant confining pressure (10 MPa). The trend in stress–strain curves of the different coal samples is roughly the same and includes a crack closure, elastic deformation, failure, and residual stage. The stress–strain curves show an obvious linear characteristic.

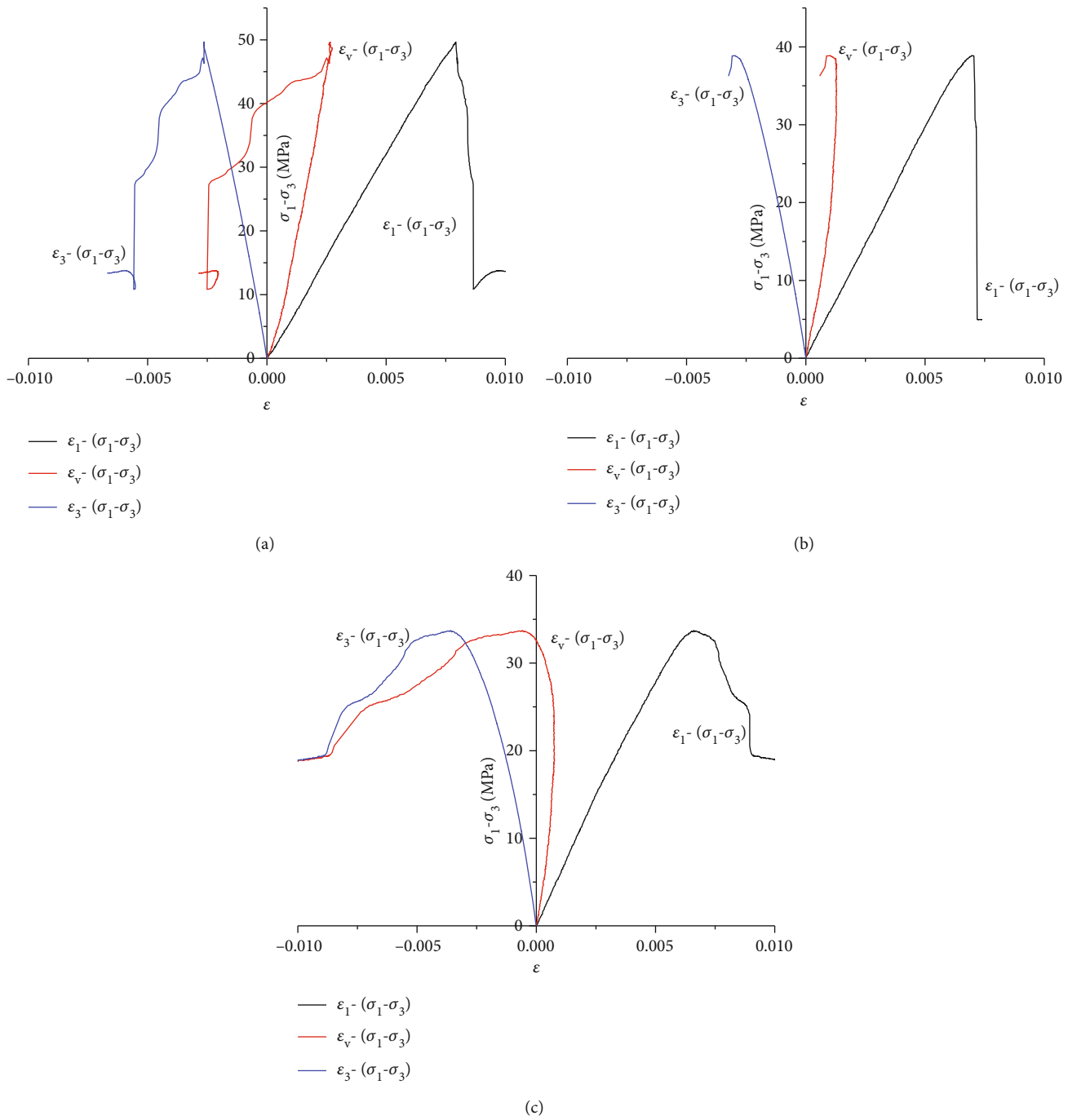

Figure 3: Triaxial test of coal samples with different beddings.

The coal sample brittleness in different bedding directions differed significantly. Compared with the bedding plane that was parallel to the axial direction, the stress–strain curve of the coal samples at angles to the axial direction decreased sharply after the peak strength was reached, which shows obvious brittle-drop characteristics. This phenomenon is more obvious in the TUT, and its failure is more sudden.

3.2. Deformation Characteristics Analysis. Compared with the traditional triaxial compressive test, regardless of the coal sample angle to the bedding planes, the brittle characteristics in the TUT showed a more obvious brittle failure sound in the test, and the stress–strain curve showed an obvious decreasing trend after the peak strength.

With the increase in axial pressure, the stress–strain curve is nearly linear in the loading stage of the TUT. The slope of the axial strain was smaller than that of the circumferential strain. The increase in circumferential strain was minimal, like that of the traditional triaxial compressive test, and the change in the volume strain was influenced mainly by the axial strain. The circumferential strain changes of the coal samples with different bedding planes made a slight

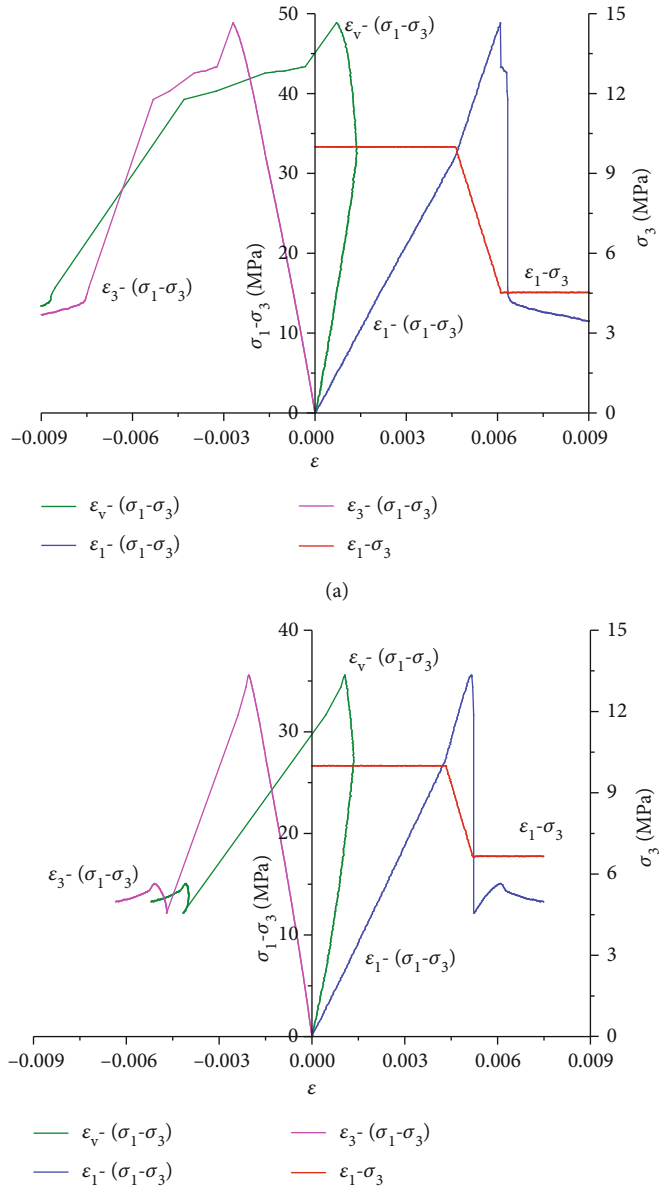

Figure 4: Continued.

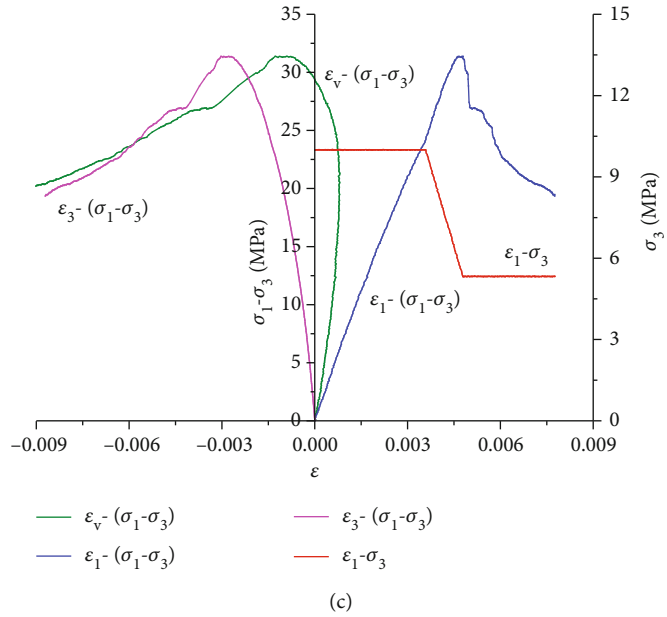

(c)

Figure 4: Unloading test of coal samples with different beddings.

Table 2: Test results of unloading and triaxial compression failure.

No.	σ_1-σ_3′ (MPa)	σ_3′ (MPa)	σ_3-σ_3′ (MPa)	ε_1 (mm/mm)	ε_3 (mm/mm)
V-S-1	48.52	—	—	0.007858	0.002635
V-S-2	53.63	—	—	0.008236	0.002963
V-S-3	49.63	—	—	0.008123	0.002852
V-X-1	47.82	5.32	4.68	0.006093	0.002592
V-X-2	45.36	6.65	3.35	0.005624	0.002501
V-X-3	46.23	5.86	4.14	0.005982	0.002526
T-S-1	38.87	—		0.006983	0.005563
T-S-2	43.26	—		0.007653	0.005687
T-S-3	40.15	—		0.007125	0.005601
T-X-1	37.21	6.26	3.74	0.005416	0.002631
T-X-2	35.60	5.20	4.80	0.005021	0.002539
T-X-3	36.01	5.22	4.78	0.005238	0.002602
P-S-1	33.67	—		0.005563	0.002922
P-S-2	38.56	—		0.006521	0.003126
P-S-3	35.63	—		0.006159	0.003096
P-X-1	31.30	4.52	5.48	0.004635	0.002731
P-X-2	29.63	4.63	5.37	0.004123	0.002601
P-X-3	30.12	5.06	4.94	0.004356	0.002698

difference. Under the application of an axial stress, cracks developed in coal samples with vertical and oblique bedding planes. The circumferential strain slope was minimal, and the circumferential deformation was obvious.

After unloading the confining pressure, the slope of the circumferential deformation increased, especially for coal samples with vertical bedding planes and oblique planes. The development law of volume strain was like the circumferential strain; the curve began to "turn left," and the slope increased. The coal samples began to swell.

As the confining pressure decreased, the load-carrying capacity decreased, and the coal samples were fractured and became unstable because of the underlying confining pressure on the sample surface and the more violent failure than that of the traditional triaxial compressive test, especially for samples with vertical and oblique bedding planes.

3.3. Strength Characteristics Analysis. Test data under different conditions are shown in Table 2. Compared with the TUT, the triaxial compressive strength of coal samples with

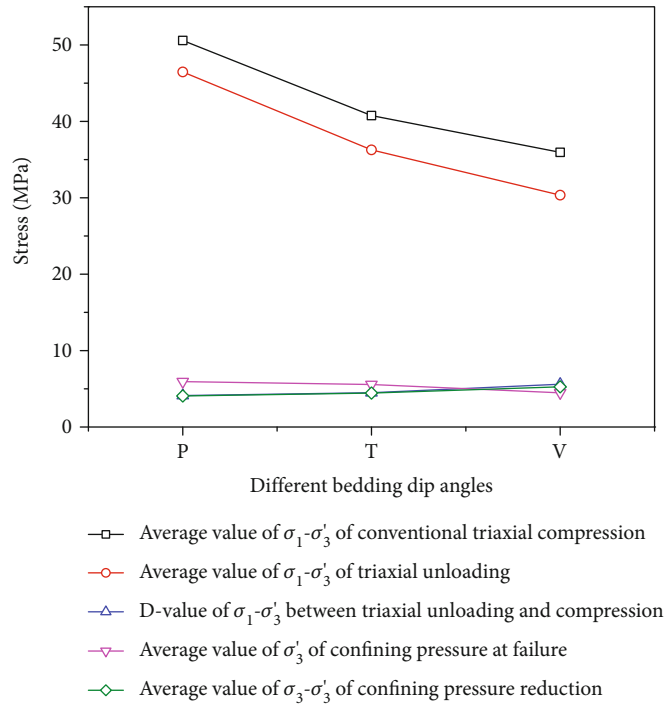

Figure 5: Comparison of test results for different layered dip coal samples.

different bedding planes was higher, which indicates that coal samples are more likely to crack under an unloading confining pressure.

The strength differences between the traditional TCST and the TUT of coal samples with different bedding planes were calculated. The average strengths of the horizontal, oblique, and vertical bedding planes were 4.12, 4.49, and 5.60 MPa, respectively. Compared with the traditional TCST, the average decreases in peak strength were 8.14%, 11.02%, and 15.58%, respectively.

The ultimate strength of coal samples with different bedding planes in traditional TCSTs and TUTs is important. In the traditional TCST, compared with that with vertical bedding planes, the average ultimate strength of coal samples with oblique bedding planes and horizontal planes decreased by 9.83 and 14.64 MPa, respectively. In the TUT, compared with that with vertical bedding planes, the average ultimate strength of coal samples with oblique bedding planes and horizontal planes decreased by 10.20 and 16.12 MPa, respectively. The average decrease in ultimate strength in the triaxial loading test exceeded that of the traditional TCST, which indicates that the unloading effect influences the strength of coal samples with bedding planes. As shown in Figure 5, it is easier for coal samples with oblique and vertical bedding planes to fail under the TUT.

4. Analysis of AE Characteristics of Bedding Coal Samples during Unloading Failure

Figure 6 compares the AE-RNT (acoustic emission ring count rate) curves of coal samples with different bedding inclinations. The regularity of different coal samples during unloading failure was similar and could be divided into a compaction, elastic–plastic, failure-during-unloading-confining-pressure, and macrofailure stage.

In the compaction stage, like the conventional triaxial compression test, primary cracks in the coal sample were closed. No AE phenomenon occurred in coal samples with bedding perpendicular to the axial loading direction. A sporadic AE phenomenon occurred in this stage in coal samples with a declining bedding, whereas the AE phenomenon was more obvious in coal samples with parallel bedding.

In the elastic–plastic stage, the early AE activity was weak. With an increase in axial stress, the internal energy accumulated and the primary cracks in the coal sample expanded, which resulted in AE activity. In this time, the ring count rate was ~300 s^{-1}. Before the unloading, the AE activity entered an active period because of massive crack initiation and propagation, and the AE-RNT multiplied in this time compared with previously.

After unloading, the confining pressure decreased gradually, and the axial load continued to increase. In this case, large-scale cracks were generated, and the AE activity was enhanced.

With the continuous increase in axial load and the decrease in confining pressure, the AE activity began to weaken, and the AE-RNT decreased significantly compared with the active period, which resulted in a short period of "relative silence." The coal sample then reached a peak stress point and entered the failure stage. In this stage, internal cracks in the coal sample began to expand rapidly, converge, and penetrate, and the AE activity increased rapidly until sudden coal sample failure. In this time, the AE-RNT and energy of the coal sample reached a maximum, and the AE was extremely active.

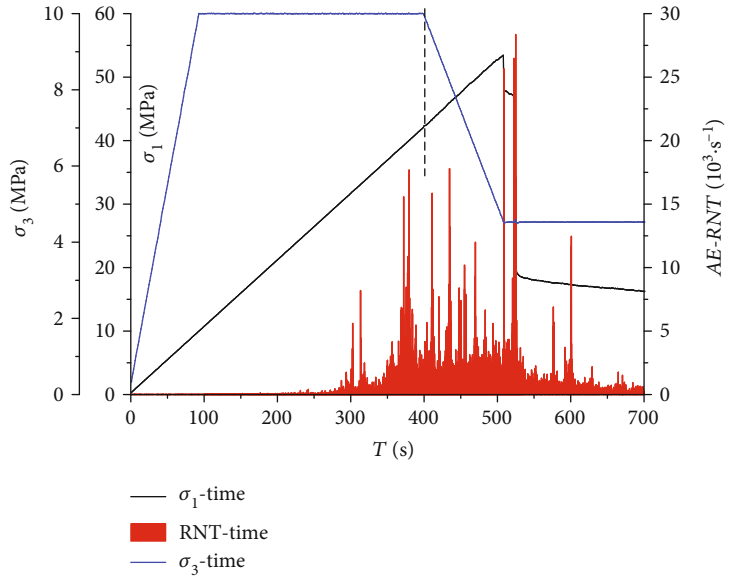

(a)

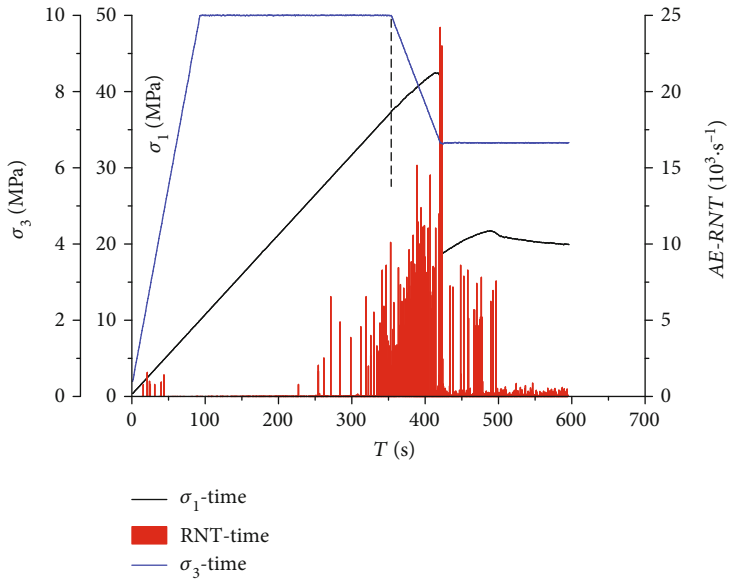

(b)

Figure 6: Continued.

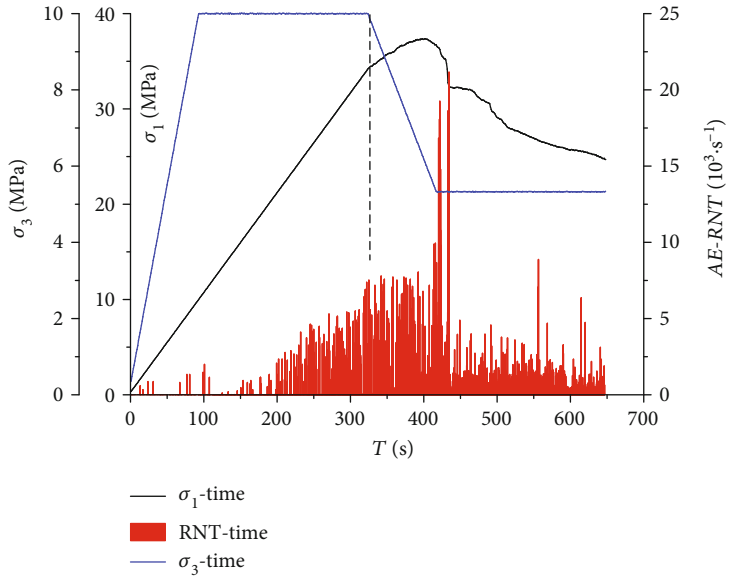

(c)

Figure 6: Test results of AE-RNT curves of rock samples under triaxial compression and unloading failure.

Different from the obvious sudden failure of coal samples with vertical bedding and inclined bedding, coal samples with parallel bedding show more ductility characteristics in the failure stage and have a longer failure stage. In coal samples with vertical and inclined bedding, the AE-RNT shows a sudden decrease in the failure stage, but in samples with parallel bedding, the AE-RNT maintains a high level for a while during the failure stage. The maximum AE-RNT varied with the bedding dip angle. The coal sample with a vertical bedding had the highest AE-RNT, followed by the coal sample with inclined and parallel bedding. The result indicates that the unloading failure degree of a coal sample with parallel bedding is more severe.

A comparison of the distribution of AE amplitude (AE-A) of coal samples with different bedding dip angles shows that coal samples with an inclined and parallel bedding have a wider distribution range of AE-A during the elastic loading stage, as shown in Figure 7. This result occurs because, in the elastic loading stage, crack propagation of the coal sample with vertical bedding was smaller, and thus, a large amount of energy accumulated. For the coal sample with inclined and parallel bedding, crack propagation occurred throughout the test.

In the TUT, the distribution range of AE-A of the coal samples with different bedding dip angles varied between 40 and 90 dB. At the beginning of the test, the AE-A and distribution range of coal sample AE-A increased gradually, but the variation was insignificant. After unloading, the distribution range of the AE-A increased significantly, and the peak AE-A gradually reached a maximum because of crack propagation. After coal sample failure, the distribution range of AE-A was basically the same as the failure stage, and the high and low amplitudes were distributed widely, which indicates that in addition to many large-scale fractures, some small-scale fractures existed in the coal sample during this stage.

5. Prediction of Unloading Failure of Coal Sample Based on Acoustic Emission Parameters

Catastrophe theory studies the catastrophe characteristics of things from a quantitative perspective and characterizes them through a unified mathematical model. At present, the main types of mutations are elliptical umbilical point mutation, dovetail mutation, cusp mutation, point mutation, hyperbolic umbilical point mutation, folding mutation, and parabolic umbilical point mutation. Cusp mutation theory, swallow tail mutation theory, and butterfly mutation theory are widely used in describing the mutation characteristics of things. In this paper, the cusp catastrophe theory is used to select the acoustic emission ring count rate for catastrophe prediction, and then, the unloading failure time of coal samples is compared with the prediction results to explore its feasibility.

5.1. Construction of Coal Sample Unloading Failure Prediction Model. As a branch of nonlinear theory, Thon first proposed catastrophe theory, which applies mathematical methods to study the law of jump change in dynamics. Without knowing the differential equation and differential equation of the system, applying catastrophe theory can predict the qualitative or quantitative state of the system with a few control variables only through a few assumptions. At present, catastrophe theory is widely used in rock engineering stability evaluation.

Through the above analysis, it can be concluded that the acoustic emission ring count rate (AE-RNT) and amplitude can better reflect the unloading damage and failure evolution process of coal samples. For coal sample unloading failure prediction, scholars mainly conduct qualitative analysis on acoustic emission parameters. This paper uses catastrophe

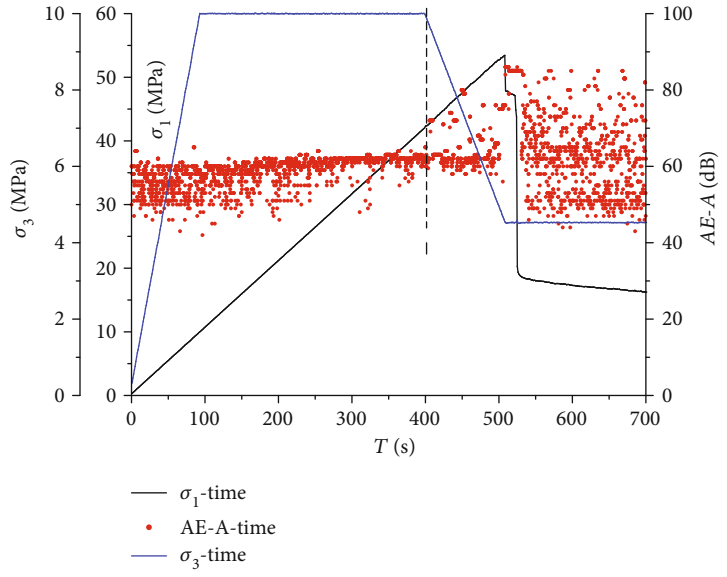

(a)

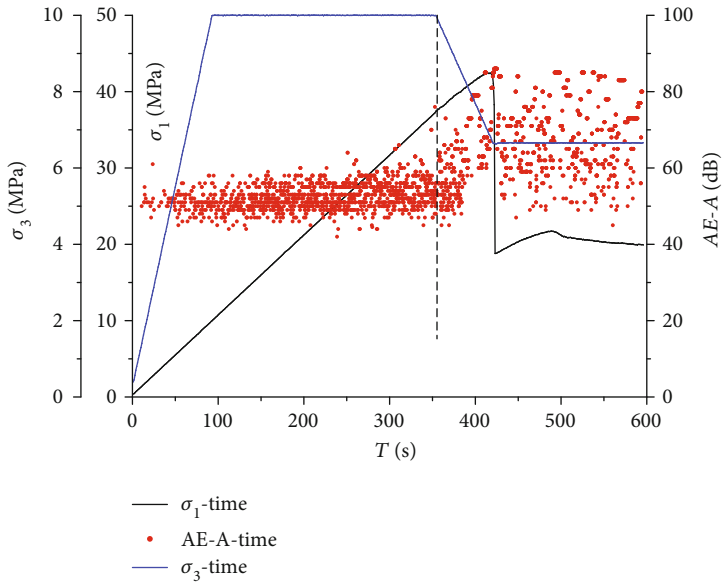

(b)

Figure 7: Continued.

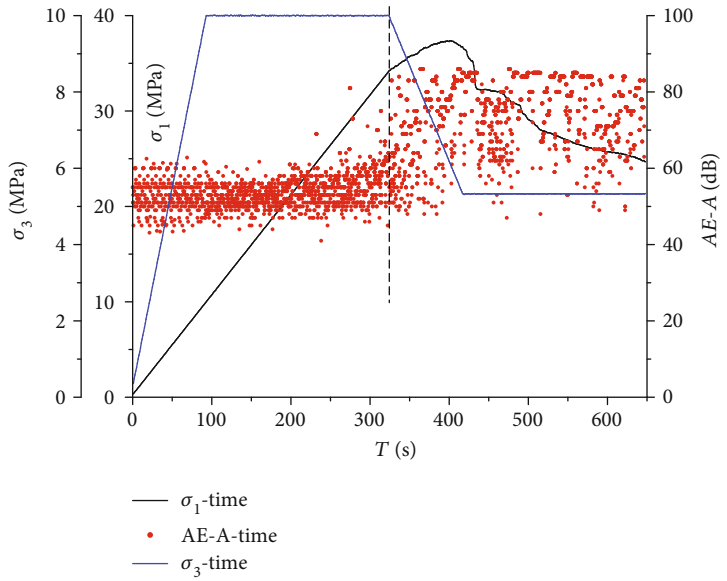

(c)

Figure 7: Test results of AE amplitude distribution of rock samples under triaxial compression and unloading failure.

theory to combine acoustic emission parameters and catastrophe theory to predict coal sample unloading failure. Taking the acoustic emission ring count rate as a continuous function U(t) of time variable (where U is the acoustic emission monitoring data sequence and t is time), the continuous function U(t) can be expanded by the Taylor series to obtain

$$\begin{aligned} U(t) = f(t) &= f(t_0) + f'(t_0)t + f''(t_0)t^2 + \cdots + f^{(m)}(t_0)t^m \\ &= a_0 + a_1 t + a_2 t^2 + a_3 t^3 + \cdots + a_m t^m. \end{aligned} \tag{1}$$

Intercept the first 5 items (i.e., intercept the 4th power item) in equation (1) and construct the cusp catastrophe model, which can be obtained as follows:

$$U(t) = a_0 + a_1 t + a_2 t^2 + a_3 t^3 + a_4 t^4. \tag{2}$$

Let $t = x - N$; when constructing the cusp catastrophe model, the x can still express the process of time, which can be brought into equation (2):

$$U(x) = b_0 + b_1 x + b_2 x^2 + b_3 x^3 + b_4 x^4, \tag{3}$$

where $b_0 = a_4 N^4 - a_3 N^3 + a_2 N^2 - a_1 N + a_0$, $b_1 = -4a_4 N^3 + 3a_3 N^2 - 2a_2 N + a_1 b_4 = a_4$, $b_3 = a_3 - 4a_4 N$, and $b_2 = 6a_4 N^2 - 3a_3 N + a_2$.

Let $b_3 = a_3 - 4a_4 N = 0$, then $N = a_3/4a_4$.

Let $U_1(x) = U_1(x)/4b_4$, $p = b_2/2b_4$, and $q = b_1/4b_4$; then, we can get

$$U_1(x) = \frac{1}{4}x^4 + \frac{p}{2}x^2 + qx + \frac{b_0}{4b_4}. \tag{4}$$

So far, the cusp catastrophe model with p and q as control variables is obtained, and its equilibrium surface equation is

$$U_1' = x^3 + px + q. \tag{5}$$

The surface consists of three layers, which are divided into the upper, middle, and lower leaves. The nonisolated setpoint needs to meet equation (5) and the following equation:

$$U_1'' = 3x^2 + p = 0. \tag{6}$$

The bifurcation set equation is

$$\Delta = 4p^3 + 27q^2. \tag{7}$$

The above formula is the instability failure criterion of the coal sample based on the acoustic emission ring count rate. When$\Delta > 0$, the coal sample is in a stable state; when$\Delta = 0$, the coal sample is in the critical state of stability and instability; and when$\Delta < 0$, the coal sample is damaged, as shown in Figure 8.

5.2. Example Analysis of Coal Sample Unloading Failure Prediction. According to the temporal and spatial evolution characteristics of acoustic emission parameters, there is an obvious quiet period before coal sample unloading failure, which provides a good condition for acoustic emission to predict coal sample unloading failure. Based on this, the monitoring data of acoustic emission parameters (ring count rate) in the quiet period is selected as the time series U(T), and the predicted results of the coal sample unloading failure are shown in Table 3.

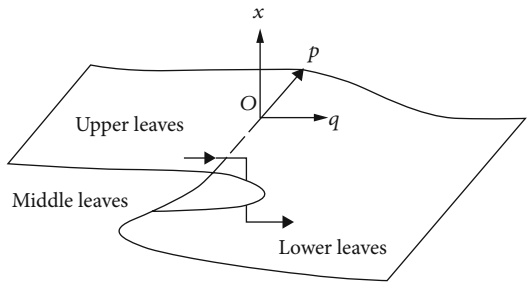

Figure 8: Catastrophe equilibrium surface.

Table 3: Acoustic emission prediction of coal sample unloading failure.

Coal sample	Parameter		
	Time when Δ = 0/s	Actual failure time (s)	Difference (s)
V-X-1	501	503.4	2.4
V-X-2	505	510.7	5.7
V-X-3	502	506.2	4.2
T-X-1	413	417.6	4.6
T-X-2	405	410.5	5.5
T-X-3	411	414.6	3.6
P-X-1	395	398.7	3.7
P-X-2	387	392.9	5.9
P-X-3	389	393.8	4.8

As can be seen from the table, the Δ value equal to zero appears before the coal sample is damaged, the difference between the value and the actual fracture time is no more than 6 s, and the average time is 4.49 s. It can be seen that although there is a slight difference in the time of predicting the unloading failure of the coal sample by using the ring count rate, it can better predict the coal sample failure on the whole. Therefore, it is feasible to predict the unloading failure of the coal sample by using acoustic emission parameters and cusp catastrophe theory.

6. Conclusions

(1) The brittle characteristic of coal samples with different bedding directions differed visibly. Compared with coal samples with parallel bedding, coal samples with vertical and inclined bedding showed a sharper decrease in the stress–strain curve after the ultimate strength of coal was reached, which indicates the strong brittle characteristic

(2) In the unloading test, the variation law of the circumferential strain of coal samples with different bedding directions differed. Cracks in the coal sample with vertical and inclined bedding expanded rapidly under an axial force. Thus, the curve slope of the circumferential strain was small, and the circumferential deformation was obvious in this case

(3) The unloading failure limit strength of coal samples with different bedding directions was different. Compared with the coal sample with a vertical bedding, the average strength of the coal sample with an inclined and parallel bedding decreased by 10.20 and 16.12 MPa, respectively, which indicates that such samples are prone to failure

(4) The variation range of the coal sample strength with different bedding directions under unloading conditions exceeded that of the conventional triaxial compression test, which indicates that the unloading effect had a more obvious impact on bedding coal sample strength. The ductility characteristic of coal samples with parallel bedding during the failure stage was more obvious

(5) The maximum AE-RNT varied with bedding direction. Coal samples with a vertical bedding had the highest AE-RNT, followed by coal samples with an inclined and parallel bedding. The result indicates that the unloading failure degree of a coal sample with parallel bedding is more severe

(6) Using the acoustic emission ring count rate and the cusp catastrophe theory, the unloading failure prediction of coal samples is carried out. The prediction results are not different from the experimental results, which shows that this method is feasible

Data Availability

The data used to support the findings of this study are available from the corresponding authors upon request.

Conflicts of Interest

The authors declare that there are no conflicts of interest related to the publication of this paper.

Acknowledgments

This research has been supported by the Opening Foundation of Shandong Key Laboratory of Civil Engineering Disaster Prevention and Mitigation (CDPM2021KF16) and the National Natural Science Foundation of China (51574156). This research was also partially funded by the Project of Shandong Province Higher Educational Science and Technology Program (J18KA195) and the Natural Science Foundation of Shandong Province (ZR2019PD016).

References

[1] K. D. Liu, Q. S. Liu, Y. G. Zhu, and B. Liu, "Experimental study of coal considering directivity effect of bedding plane under Brazilian splitting and uniaxial compression," *Chinese Journal of Rock Mechanics and Engineering.*, vol. 32, no. 2, pp. 308–316, 2013.

[2] X. H. Liu, F. Dai, J. F. Liu, and R. Zhang, "Brazilian splitting tests on coal rock considering bedding direction under static and dynamic loading rate," *Chinese Journal of Rock Mechanics and Engineering.*, vol. 34, no. 10, pp. 2098–2105, 2015.

[3] D. Xu, R. Zhang, M. Z. Gao et al., "Research on coal bedding effect based on indirect tensile test," *Journal of China Coal Society*, vol. 42, no. 12, pp. 3133–3141, 2017.

[4] P. Hou, F. Gao, Y. Yang, Z. Zhang, and X. Zhang, "Effect of bedding orientation on failure of black shale under Brazilian tests and energy analysis," *Chinese Journal of Geotechnical Engineering*, vol. 38, no. 5, pp. 930–937, 2016.

[5] P. Hou, F. Gao, Y. G. Yang et al., "Effect of bedding plane direction on acoustic emission characteristics of shale in Brazilian tests," *Rock and Soil Mechanics*, vol. 37, no. 6, pp. 1603–1612, 2016.

[6] J. Y. Teng, J. X. Tang, Y. N. Zhang, J. C. Duan, and J. B. Wang, "Damage process and characteristics of layered water-bearing shale under uniaxial compression," *Rock and Soil Mechanics*, vol. 38, no. 6, pp. 1629–1638, 2017.

[7] J. Y. Teng, Y. N. Zhang, J. X. Tang, C. Zhang, and C. L. Li, "Mechanical behaviors of anchored bedding rock under uniaxial compression," *Rock and Soil Mechanics*, vol. 38, no. 7, pp. 1974–1982, 2017.

[8] X. Ren, H. Hang, and X. Zhang, "Study of effects of bedding structure on uniaxial mechanical properties of coal rock," *Journal of China Coal Society*, vol. 36, no. 1, pp. 63–65, 2017.

[9] Z. P. Zhang, R. Zhang, Z. T. Zhang, M. Z. Gao, and F. Dai, "Experimental research on effects of bedding plane on coal acoustic emission under uniaxial compression," *Chinese Journal of Rock Mechanics and Engineering*, vol. 34, no. 4, pp. 770–778, 2015.

[10] Z. Q. Yang, W. X. Deng, P. H. Zhang, P. T. Wang, T. W. Zhang, and T. H. Yang, "The influence of bedding angle on acoustic emission characteristics in biotite granulite," *Journal of Mining & Safety Engineering*, vol. 33, no. 3, pp. 521–527, 2016.

[11] Q. Sun, Z. Z. Zhang, and L. Du, "Effect of bedding angle on mechanical and acoustic emission characteristics of layered rock," *Metal Mine*, vol. 2, pp. 7–13, 2017.

[12] B. Xie, X. Wang, and P. Lv, "Dynamic properties of bedding coal and rock and the SHPB testing for its impact damage," *Journal of Vibration and Shock*, vol. 36, no. 21, pp. 117–124, 2017.

[13] J. Pei, J. Liu, and J. Xu, "Experimental study of mechanical properties of layered marble under unloading condition," *Chinese Journal of Rock Mechanics and Engineering.*, vol. 8, no. 12, pp. 2496–2502, 2009.

[14] H. F. Deng, W. Wang, J. L. Li, Y. C. Zhang, and X. J. Zhang, "Experimental study on anisotropic characteristics of bedded sandstone," *Chinese Journal of Rock Mechanics and Engineering.*, vol. 37, no. 1, pp. 112–120, 2018.

[15] Y. C. Li, X. F. Ma, N. Li et al., "Experimental study on influence of bedding planes on stimulation effect of hydraulic fracturing in shale reservoir," *Journal of Xi'an Shiyou University(Natural Science Edition)*, vol. 32, no. 5, pp. 62–67, 2017.

[16] H. T. Liu, H. Zhou, D. W. Hu, C. Q. Zhang, C. K. Qu, and Y. C. Tang, "Experiment study of thermal expansion coefficient of sandstone with beddings," *Rock and Soil Mechanics*, vol. 38, no. 10, pp. 2841–2846, 2017.

[17] Y. M. Song, T. Z. Xing, T. B. Zhao, Z. X. Zhao, and P. B. Gao, "Acoustic emission characteristics of deformation field development of rock under uniaxial loading," *Chinese Journal of Rock Mechanics and Engineering*, vol. 36, no. 3, pp. 534–542, 2017.

[18] Y. B. Zhang, G. Yu, and B. Tian, "Identification of multiple precursor information of acoustic emission dominant frequency in the process of granite failure," *Journal of Mining & Safety Engineering*, vol. 34, no. 2, pp. 355–362, 2017.

[19] S. Li, X. Cheng, C. Liu, C. Cheng, and M. Y. Yang, "Damage characteristics and space-time evolution law of rock similar material under uniaxial compression," *Journal of China Coal Society*, vol. 42, Suppl.1, pp. 104–111, 2017.

[20] X. L. Liu, M. C. Pan, X. B. Li, and J. P. Wang, "Acoustic emission b-value characteristics of granite underdynamic loading and static loading," *Chinese Journa of Rock Mechanics and Engineering*, vol. 36, Suppl.1, pp. 3148–3155, 2017.

[21] D. M. Zhang, X. Bai, G. Z. Yin, S. Li, and Q. He, "Analysis of acoustic emission parameters and energy dissipation characteristics and damage evolution of bedding rock failure process under uniaxial compression," *Journal of China Coal Society*, vol. 43, no. 3, pp. 646–656, 2018.

[22] X. L. Yao, Y. B. Zhang, X. X. Liu, P. Liang, and L. Sun, "Optimization method for key characteristic signal of acoustic emission in rock fracture," *Rock and Soil Mechanics*, vol. 39, no. 1, pp. 375–384, 2018.

[23] P. H. Zhang, T. H. Yang, T. Xu, Q. L. Yu, J. R. Zhou, and Y. C. Zhao, "The evolution law of acoustic emission events during the fracture process of altered granite gneiss," *Rock and Soil Mechanics*, vol. 38, no. 8, pp. 2189–2197, 2017.

[24] Y. Yang, Y. Zhou, D. Ma, H. Ji, and Y. Zhang, "Acoustic emission characteristics of coal under different triaxial unloading conditions," *Acta Geodynamica et Geromaterialia*, vol. 17, no. 1, pp. 51–61, 2020.